Available online at www.sciencedirect.com
ScienceDirect
Journal of Organometallic Chemistry 693 (2008) 1058–1064
Journal of Organometallic Chemistry
www.elsevier.com/locate/jorganchem

Evaluating the kinetic indenyl effect of a π-thiaphentalenyl ancillary ligand

Denis A. Kissounko [a,b,*], Maxim V. Zabalov [b], Neil M. Boag [a], Yurii F. Oprunenko [b], Dmitri A. Lemenovskii [b]

[a] *Department of Chemistry and Applied Chemistry, University of Salford, Salford M5 4WT, UK*
[b] *Moscow State University, Chemistry Department, Vorob'evy Gory, Moscow 119899, Russia*

Received 14 September 2007; received in revised form 19 December 2007; accepted 20 December 2007
Available online 28 December 2007

Abstract

The magnitude of the "kinetic indenyl effect" for the π-thiapentalenyl ligand, isoelectronic heteroanalogue of the indenyl ligand, has been tested using the reaction between complex, Rh(η^5-th)$(CO)_2$ **3** (th = 2-ethyl-5-methyl-cyclopenta[*b*]thienyl or thiapentalenyl) and PPh_3 as a model process. Only moderate "kinetic indenyl effect" of the thiapentalenyl ligand was observed. The rational for such behavior was also supported by DFT computational correlation of ground and transition states for the reaction of carbonyl group substitution by a phosphine in the corresponding indenyl and thiapentalenyl rhodium complexes.

Keywords: Kinetic indenyl effect; Thiapentalenyl ligand; Rhodium

1. Introduction

Organometallic complexes with indenyl ancillary ligand have received considerable attention over the past two decades for the reasons of their enhanced catalytic activity in olefin polymerization processes [1–3] as well as fundamental structure/properties relationship studies [4]. Part of the rational for the elevated interest into indenyl ligand-containing species can be attributed to the "kinetic indenyl effect" first described by Mawby et al. [5,6] followed by extensive work by Basolo et al. for a series of indenyl and cyclopentadienyl rhodium derivatives [7–11], which defined the significant kinetic rate enhancement for the substitution of ancillary ligands in indenyl *versus* cyclopentadienyl organometallic derivatives [12]. Such enhancement is commonly attributed to much easier indenyl ring slippage from η^5- to η^3-bonding mode (resonance structures **I** and **II** at Chart 1) with a metal leading to much faster ancillary ligand substitution via associative mechanism *versus* a dissociative pathway for the corresponding cyclopentadienyl analogues [13]. The alternative argument to this is that the enhanced substitution reactivity of indenyl species compared to their cyclopentadienyl analogues may arise from a ground rather than transition state effect (*i.e.* from a weaker bonding of indenyl ligand to the metal compared to cyclopentadienyl analogue), since many indenyl complexes exhibit considerable distortion from an ideal η^5-geometry [14]. It has also been shown that ligand substitution in indenyl complexes can occur through η^1-intermediates [15].

In a wake of extensive research into organometallic indenyl species there has been a growing number of reports of complexes with aza- and thia-heterocyclic ligands, isolectronic to the π-indenyl ligand, which also have demonstrated enhanced catalytic activity in α-olefin polymerization processes when compared to the related carboanalogues [16–24]. However, the paucity of isolated

* Corresponding author. Present address: Center for Composite Materials, University of Delaware, Newark, DE 19716, United States. Tel.: +1 302 831 0376.
E-mail address: kissounk@udel.edu (D.A. Kissounko).

0022-328X/$ - see front matter © 2008 Published by Elsevier B.V.
doi:10.1016/j.jorganchem.2007.12.027

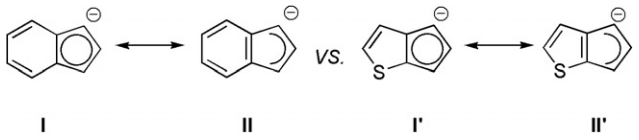

Chart 1.

organometallic species with such ligands have precluded any relevant fundamental reactivity studies of a heterocyclic ligand. We have recently synthesized a number of new organometallic derivatives of σ-and π-bonded 2-ethyl-5-methyl-cyclopenta[*b*]thienyl (or otherwise thiapentalenyl) and 4H-cyclopenta[2,1-b:3,4-b′]dithiophene (or otherwise thiafluorenyl) ligands [25–27]. In continuation of our thiapentalenyl ligand fundamental reactivity studies we now report the evaluation of its "kinetic indenyl effect" (*i.e.* $\eta^5 \rightarrow \eta^3$-thiapentalenyl ring slippage as illustrated by structures **I′** and **II′** at Chart 1) by means of kinetic and computational DFT studies following the carbonyl group substitution reaction by a phosphine in a rhodium complex, Rh(η^5-Th)$(CO)_2$ **3**, as a convenient model system, and direct correlation of the data with related carbocyclic indenyl analogues.

2. Experimental

2.1. General considerations

All syntheses were performed under an atmosphere of dinitrogen. Standard Schlenk techniques were used for the preparation of organometallic compounds. Liquids were transferred by means of steel catheters through suba seal fittings or by syringe.

Solvents were freshly distilled from sodium/benzophenone (THF) and sodium/potassium alloy (hexane). Isomeric 2-ethyl-5-methyl-6*H*-cyclopenta[*b*]thiophene and 2-ethyl-5-methyl-4*H*-cyclopenta[*b*]thiophene (as a 7:3 mixture, respectively) [28,29], and $[Rh(CO)_2Cl]_2$ [30], were prepared according to the literature methods. All other reagents were used as supplied.

Infrared spectra were recorded on a Perkin–Elmer 1710 Fourier Transform spectrometer using CaF_2 solution cells fitted with Luer lock taps. UV measurements were performed on Agilent 8453 UV–Vis spectrometer. NMR spectra were recorded a Bruker AC-300 spectrometer (^{1}H at 300.13 MHz and $^{13}C\{^1H\}$ at 75.47 MHz, referenced to $SiMe_4$). All spectra were recorded at ambient temperatures.

Column chromatography was undertaken using intermediate activity silica (Grade 4).

Microanalysis was carried out by the microanalysis group at Moscow State University.

2.2. Synthesis of 3

To a mixture of isomeric **1a** and **1b** (0.16 g, 1 mmol) in 20 ml of THF, 0.4 ml of 1.5 M *n*-BuLi was added at −20 °C. After stirring overnight at ambient temperature, 0.1 g (0.257 mmol) of $[Rh(CO)_2Cl]_2$ was added to the solution of the lithium salt **2** and the reaction mixture was stirred at the ambient temperature for another 16 h. The solvent was then removed *in vacuo* and the residue extracted into hexane. A stream of CO was flushed through the solution for 30 min to convert any traces of $Rh_2(\eta^5$-th$)_2(CO)_3$ into **3**, whereupon the solution color gradually turned from brown to red. The solution was concentrated *in vacuo* and passed through a short column of silica gel using hexane as the eluent. The first band of organic impurities was rejected. The second red-brown band containing both **3** and the dimer, $[Rh_2(\eta^5$-th$)_2(CO)_3]$, was collected, the volume reduced to *c.a.* 10 ml and a stream of CO was passed through the solution once again. Then all the volatiles were removed *in vacuo* and the residue was re-crystallized from a small amount of hexane at −20 °C and dried in high vacuum to afford 0.073 mg (61%) of **3** as red solid.

^{1}H NMR (C_6D_6, numbering according to the heterocyclic nomenclature): δ 0.95 (t, 3H, $^3J = 7.5$ Hz, CH_3CH_2), 1.78 (s, 3H, Me), 2.35 (q, 2H, $^3J = 7.5$ Hz, CH_3CH_2), 4.98 (s, 1H, H4), 5.02 (s, 1H, H6), 6.08 (s, 1H, H3). $^{13}C\{^1H\}$ NMR (C_6D_6): δ 15.1 (CH_3CH_2), 15.7 (Me), 24.5 (CH_3CH_2), 73.9 (C4), 75.02 (C6), 112.1 (C3), 115.2 (C8), 119.0 (C5), 122.5 (C7), 149.1 (C2), 192.2 (d, $^1J_{RhC} = 85$ Hz, CO). IR (hexane, cm^{-1}): 2040, 1980 (CO). Elemental Anal. Calc. for $C_{12}H_{11}O_2RhS$: C, 44.74; H, 3.44. Found: C, 44.27; H, 3.24%.

2.3. Kinetic measurements of the reaction between 3 and PPh_3

A solution of PPh_3 of appropriate concentration in toluene was added to a quartz cell adapted for air sensitive operations filled with nitrogen. The cell was placed in thermostated cell holder and allowed to equilibrate at 25 °C. An aliquot of 7 μl of 1.7 mM solution of complex **3** in toluene was added to the well-stirred solution of PPh_3. Rate constants were determined by monitoring the increase in absorption of monosubstituted phosphine derivative **4** at $\lambda_{max} = 365$ nm. The correlation coefficient of the least-squares line ($R^2 > 0.998$) was very good with the intercept very close to zero (1.6×10^{-6}). All the experiments were carried out under pseudo-first-order conditions with a greater than tenfold excess of phosphine, and went to a 100% conversion of the starting complex **3**. No other byproducts were detected by either IR or NMR spectroscopy of crude reaction mixture.

2.4. Isolation of 4

Combined solutions left over from kinetic studies of reaction between **3** and PPh_3 were concentrated under vacuum to a volume of *c.a.* 1 ml, whereupon the entire mixture was transferred to a chromatography column packed with silica and eluted with a toluene/hexane 3:1 mixture. The single orange bang was collected and stripped to dryness yielding to **4** as an orange solid.

^{1}H NMR (C_6D_6): δ 1.07 (t, 3H, $^3J = 7.5$ Hz, CH_3CH_2), 1.45 (s, 3H, Me), 2.46 (q, 2H, $^3J = 7.5$ Hz, CH_3CH_2), 4.94 (s, 1H, H4), 5.18 (d, 1H, $J_{PH} = 3$ Hz, H6), 6.22 (d, 1H, $J_{PH} = 5$ Hz, H3), 6.92–7.86 (m, 15H, PPh_3). $^{13}C\{^1H\}$ NMR (C_6D_6): δ 15.1 (CH_3CH_2), 16.2 (Me), 23.8 (CH_3CH_2), 72.9 (C4), 75.02 (C6), 112.1 (C3), 115.2 (C8), 119.0 (C5), 121.8 (C7), 123–154 (C2, PPh_3), 197.2 (dd, $^1J_{RhC} = 85$ Hz, $^2J_{PC} = 20.6$ Hz, CO). $^{31}P\{^1H\}$ NMR (C_6D_6): d 52.1 (d, $^1J_{RhP} = 198$ Hz). IR (hexane, cm^{-1}): 1948 (CO). Elemental Anal. Calc. for $C_{29}H_{26}OPRhS$: C, 62.59; H, 4.71. Found: C, 62.97; H, 4.84%.

2.5. Computational procedures

Density functional (DFT) study was carried out using the *ab initio* generalized gradient approximation and the mPBE [31] or PBE [32,33] functionals with the TZ2P basis set and Priroda software [34,35]. Geometry optimization was carried out for all stable compounds and for the structures corresponding to the saddle points (in the case of transition states, **TS**). The types of the stationary points were confirmed by the vibrational frequency analysis. For the saddle points, the reaction coordinates were also calculated. All computations were performed for the gas phase.

3. Results and discussion

A mixture of isomeric **1a** and **1b** readily reacts with *n*-BuLi in THF generating the lithium salt **2**, followed by addition of $[Rh(CO)_2Cl]_2$ to afford Rh(η^5-th)$(CO)_2$ **3** as a red solid in 61% yield (Scheme 1).

Isolated complex **3** was identified by IR- and NMR spectroscopy. Also, a reaction mixture solution shows the presence of second minor species, which was tentatively identified as a dimeric complex, $[Rh_2(\eta^5\text{-th})_2(\mu\text{-CO})(CO)_2]$, by comparison of its IR-spectrum stretches (1971, 1842 cm^{-1}, THF). Such spectroscopic pattern matches characteristics of the corresponding indenyl derivative $Rh_2(\eta^5\text{-Ind})_2(\mu\text{-CO})(CO)_2$ [36]. Upon passing CO gas through the reaction mixture solution such species quantitatively convert into **3**; hence no attempts were made to isolate this minor impurity.

To elucidate the magnitude of "kinetic indenyl effect" of the π-thiapentalenyl moiety, system heteroatom on the reactivity of the metal center, kinetics of CO substitution in **3** using PPh_3 as a nucleophile have been studied. The conditions were identical to those described by Rerek and Basolo [9] for the series of related indenyl and cyclopentadienyl rhodium complexes. The reaction was followed by an increase in intensity of a UV/Vis absorption band of the monosubstituted phosphine complex **4** ($\lambda_{max} = 365$ nm, toluene). The experiments were carried out under pseudo-first-order conditions using a ten fold or greater excess of phosphine. All the reactions were run to completion. Good first-order plots were obtained with a linear dependence of the pseudo-first rate constants k_{obs} on the concentration of phosphine (Fig. 1) giving a second-order rate constant of $9.8 \times 10^{-3}\ M^{-1}\ s^{-1}$.

Although the rate observed ($9.8 \times 10^{-3}\ M^{-1}\ s^{-1}$) shows moderate rate enhancement compared to the corresponding value for Rh(η^5-Cp)$(CO)_2$ ($1.3 \times 10^{-4}\ M^{-1}\ s^{-1}$) [10], it is nowhere near the magnitude exhibited by Rh(η^5-Ind)$(CO)_2$ ($2.8 \times 10^{4}\ M^{-1}\ s^{-1}$) measured at 25 °C [9]. In fact, it is closer to the moderate rate enhancement afforded by the dimethylamino group in Rh(η^5-Me_2NCp)$(CO)_2$ ($1.05 \times 10^{-3}\ M^{-1}\ s^{-1}$ at 25 °C), which was attributed to resonance stabilisation of a η^3-intermediate by the nitrogen non-bonding electron pair [10]. Such mechanism is also plausible for the sulfur heterocycle, and the data suggest that aromatisation of the thiophene ring (*i.e.* the indenyl effect as shown in Chart 1) plays little part in the substitution chemistry of complexes containing such heterocyclic system.

To further confirm the difference in "kinetic indenyl effect" between indenyl and thiapentalenyl ligands, DFT calculations were performed for reaction 2 (Scheme 1) and related reaction with Rh(η^5-Ind)$(CO)_2$ using PMe_3 as a model reactant. The connections between stationary points in Fig. 2 were established according to IRC calculations. For comparison the geometries were optimized in two functional (mPBE and PBE). Difference between two functionals was not significant.

Thus, two different directions for a phosphine approach, *i.e. endo*- and *exo*-, give rise to two possible transition states: **TS I** and **TS II** for indenyl ligand *versus* **TS I′** and

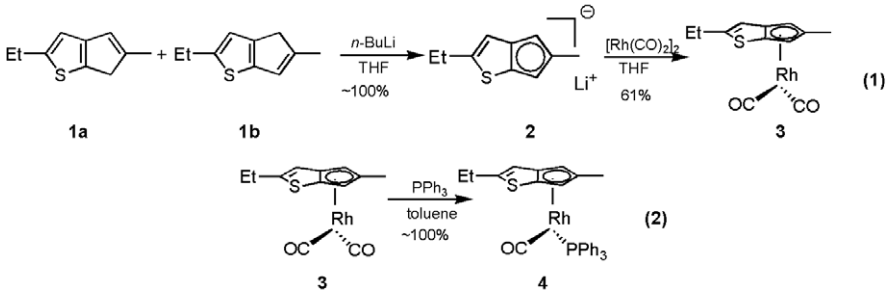

Scheme 1. Synthesis of complex **3** and CO substitution reaction by a phosphine.

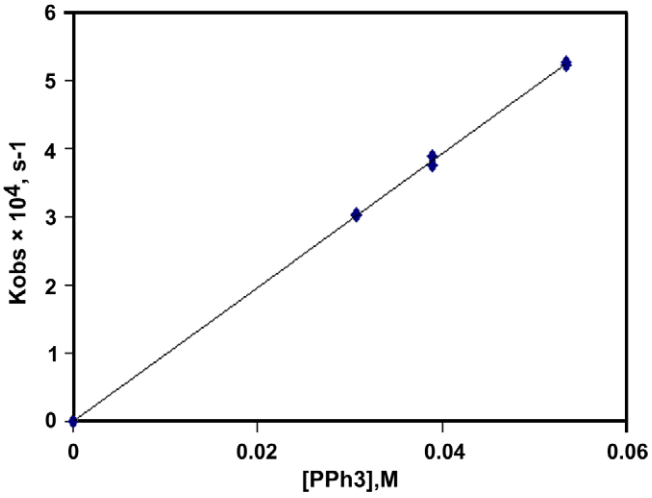

Fig. 1. Plot of k_{obs} *vs.* the concentration of PPh_3, 25 °C, toluene.

Table 1
Calculated bond lengths (Å) and angles (°) for intermediates **B** and **C**

Atoms	Distance		Atoms	Angle	
	B	**C**		**B**	**C**
Rh–C(1)	2.316	3.291	Rh–C(9)–O(1)	177.7	169.6
Rh–C(2)	2.150	2.510	Rh–C(10)–O(2)	177.5	171.8
Rh–C(3)	2.313	2.236	C(1)–Rh–C(2)	37.4	23.0
Rh–C(8)	3.000	3.625	C(1)–C(2)–C(3)	105.3	109.8
Rh–C(9)	2.998	3.116	C(2)–Rh–C(3)	37.4	35.3
Rh–C(10)	1.932	1.950	C(2)–C(1)–C(7)	107.8	108.9
Rh–C(11)	1.933	1.915	C(2)–C(3)–C(8)	107.8	105.3
C(10)–O(1)	1.160	1.159	C(9)–Rh–C(10)	94.7	140.7
C(11)–O(2)	1.160	1.164			

Table 2
Calculated bond lengths (Å) and angles (°) for intermediates **B′** and **C′**.

Atoms	Distance		Atoms	Angle	
	B′	**C′**		**B′**	**C′**
Rh–C(1)	2.231	3.353	Rh–C(10)–O(1)	179.4	170.6
Rh–C(2)	2.742	2.527	Rh–C(11)–O(2)	174.0	171.8
Rh–C(3)	3.621	2.236	C(1)–Rh–C(2)	32.6	22.3
Rh–C(7)	3.131	3.644	C(1)–C(2)–C(3)	110.4	109.9
Rh–C(8)	3.828	3.122	C(2)–Rh–C(3)	19.5	35.1
Rh–C(9)	1.907	1.948	C(2)–C(1)–C(8)	103.0	107.3
Rh–C(10)	1.949	1.915	C(2)–C(3)–C(9)	108.5	105.0
C(9)–O(1)	1.161	1.159	C(10)–Rh–C(11)	91.9	143.2
C(10)–O(2)	1.152	1.164			

TS II′ for thiaanalogue (Fig. 2, Table 1). Although the *exo*-approach pathway cannot be completely overruled, especially under thermodynamically controlled reaction, the *endo*-attack seems to be much more preferential under kinetic control, since it requires the lowest activation energy. The rational for such *endo*-regioselective attack, which was also observed recently for cationic rhodium indenyl derivatives [37], was explained earlier by the relative *trans*-effects of indenyl, carbonyl and phosphine ligands, where the ligand with the highest *trans*-effect (CO) is *trans*-position to the six-membered ring [38] (see Table 2).

Both ground states **A** and **A′** exhibit distorted η^5- or $\eta^3+\eta^2$-coordination of indenyl and thiapentalenyl ligands, respectively, to the rhodium with the corresponding bond distances of 2.270 Å [Rh–C(1)], 2.274 Å [Rh–C(2)], 2.270 Å [Rh–C(3)], 2.517 Å [Rh–C(4)], 2.517 Å [Rh–C(5)] for complex **A**; and 2.284 Å [Rh–C(1)], 2.285 Å [Rh–C(2)], 2.278 Å [Rh–C(3)], 2.498 Å [Rh–C(4)], 2.479 Å [Rh–C(5)] for complex **A′**. The following attack by a phosphine on molecules **A** and **A′** leads to both indenyl and thiapentalenyl rings slippage. The earlier work by Ceccon et al. rationalized the $\eta^5 \rightarrow \eta^3$ indenyl ligand slippage in rhodium complexes upon the attack by a nucleophile in terms of MO interactions and difined the least motion pathway for a nucleophilic species approach to the metal center [39]. Thus, of particular interest is the observation that whereas the substitution in $Rh(\eta^5\text{-Ind})(CO)_2$ occurs through postulated $\eta^5 \rightarrow \eta^3$ indenyl ligand slippage leading to the intermediate **B**, the corre-

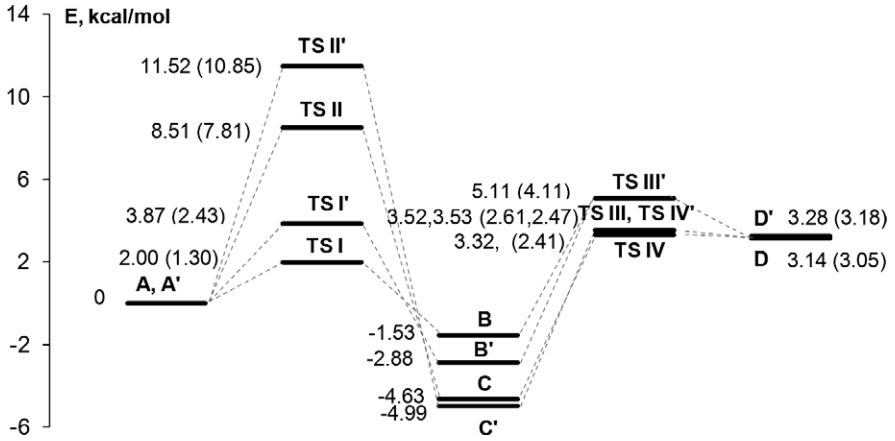

Fig. 2. Energy profile for CO to phosphine ligand substitution in indenyl and thiapentalenyl complexes derived from DFT/mPBE or DFT/PBE (in parenthesizes) calculations.

sponding reaction for the thiaanalogue leads to the intermediate **B′**, where the ancillary ligand is essentially η^1-bound to the rhodium (Fig. 2, Table 1). Accordingly, for the η^1-type intermediate **B′** Rh–C(1), Rh–C(2) and Rh–C(3) bond distances of 2.231, 2.742 and 3.621 Å, respectively, differ significantly from those for the analogous

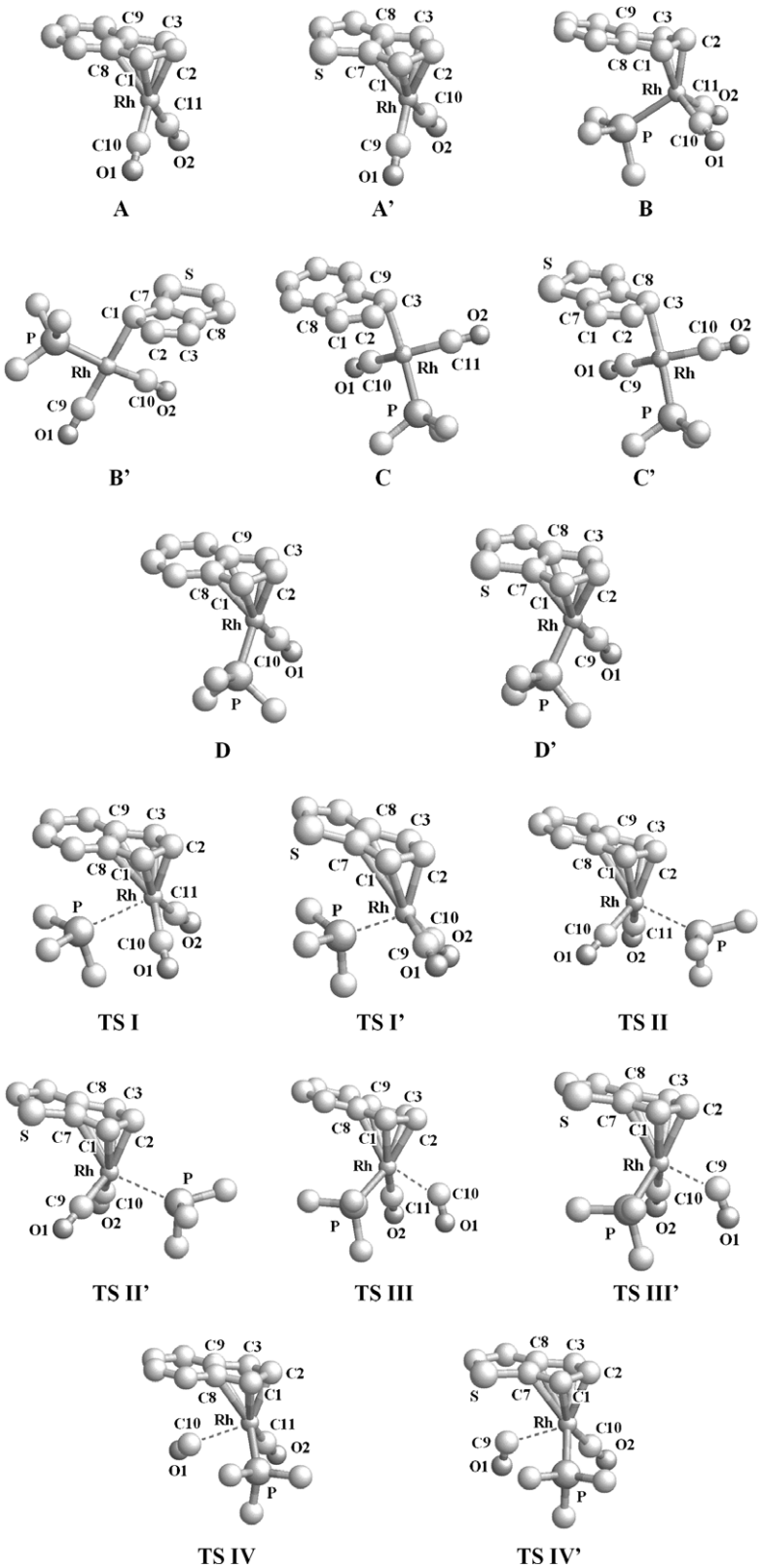

Fig. 3. Structures of transition states (TS) and intermediates for the reaction between indenyl and thiapentalenyl rhodium complexes with phosphine.

η^3-type indenyl species **B** [Rh–C(1) 2.316 Å, Rh–C(2) 2.150 Å and Rh–C(3) 2.313 Å], which represent almost undistorted allylic moiety. Also, in **B′** the Rh–C(11)–O(2) moiety (174.0°) is considerably tilted away from almost linear geometry as in indenyl analogue **B** [Rh–C(10)–O(2) 177.5°]. Hence, such $\eta^5 \rightarrow \eta^1$ observed in **A′** → **B′** pathway ring slippage requires more energy to occur, slowing down the kinetic rate of the process. Also, the diagram unambiguously shows that the differences in "kinetic indenyl effect" for complex **3** and the indenyl analogue, Rh(η^5-Ind)$(CO)_2$, can be attributed to higher energy of both transition states for the thiapentalenyl ligand complex [3.87 kcal/mol (**TS I′**) *versus* 2.0 kcal/mol (**TS I**), and 5.11 kcal/mol (**TS III′**) *versus* 3.29 kcal/mol (**TS III**)], whereas energies corresponding to the intermediate molecules (**B** and **B′**) and final products (**D** and **D′**) lie within a smaller range. Although the energy differences found for indenyl and thiapentalenyl intermediates and transition states (Fig. 3) are not large enough to be solely responsible for the dramatic difference of the indenyl effect in corresponding rhodium dicarbonyl derivatives, they clearly bear a pivotal role in reactivity decline for species **3** *versus* the corresponding indenyl analogue. We also speculate that additional weak interactions between the sulfur heteroatom and a metal center in **3** can influence the reactivity of carbonyl groups in the later complex. Both experimental and computational studies have been launched to further investigate this hypothesis, and the results will be reported elsewhere.

4. Conclusions

The data reported here significantly advance our understanding of the role played by a heteroatom in a π-bound ligand on the reactivity of other ancillary ligands at the metal center. Thus, it appears that the rate enhancement for the substitution of other ancillary ligands in a metal's coordination sphere caused by the thiapentalenyl ligand ring slippage (*i.e.* kinetic indenyl ligand effect) is negligible compared to the isoelectronic indenyl ligand. Moreover, as has been shown by DFT computational studies the substitution reaction for complex **3** occurs via more energy consuming pathway involving η^1-intermediate **B′**, whereas the reaction between phosphine and **3** goes $\eta^5 \rightarrow \eta^3$ through the conventional η^3-intermediate **B**. Although further work is necessary to elucidate whether the sulfur heteroatom can interact directly with a metal center influencing the reactivity of other ancillary ligands, the results if this study clearly highlight the reduced reactivity of ancillary ligands in π-coordinated thiapentalenyl ligand-containing organometallic species compared to isoelectronic indenyl-containing analogues. The moderate rate enhancement for thiapentalenyl rhodium derivatives was found comparable to the substituted cyclopentadienyl rhodium analogues.

Acknowledgements

The financial support from Russian Foundation for Basic Research (RFBR #98-03-32995) and the University of Salford is gratefully acknowledged.

References

[1] G.W. Coates, Chem. Rev. 100 (2000) 1223.
[2] L. Resconi, L. Cavallo, A. Fait, F. Piemontesi, Chem. Rev. 100 (2000) 1253.
[3] S. Lin, R.M. Waymouth, Acc. Chem. Res. 35 (2002) 765.
[4] M.J. Calhorda, L.F. Veiros, Coord. Chem. Rev. 230 (2002) 37.
[5] A.J. Hart-Davis, R.J. Mawby, J. Chem. Soc. A (1969) 2403.
[6] C. White, R.J. Mawby, A.J. Hart-Davis, Inorg. Chim. Acta 4 (1970) 441.
[7] M.E. Rerek, L.-N. Ji, F. Basolo, J. Chem. Soc., Chem. Commun. (1983) 1208.
[8] L.-N. Ji, M.E. Rerek, F. Basolo, Organometallics 3 (1984) 740.
[9] M.E. Rerek, F. Basolo, J. Am. Chem. Soc. 106 (1984) 5908.
[10] M. Cheong, F. Basolo, Organometallics 7 (1988) 2041.
[11] A.K. Kakkar, N.J. Taylor, T.B. Marder, J.K. Shen, N. Hallinan, F. Basolo, Inorg. Chim. Acta 198–200 (1992) 219.
[12] F. Basolo, Polyhedron 9 (1990) 1503.
[13] J.M. O'Connor, C.P. Casey, Chem. Rev. 87 (1987) 307.
[14] M.J. Calhorda, L.F. Veiros, Coord. Chem. Rev. 185 (1999) 37.
[15] C.P. Casey, T.E. Vos, J.T. Brady, R.K. Hayashi, Organometallics 22 (2003) 1183.
[16] H. Volz, R. Draese, Tetrahedron Lett. (1975) 3209.
[17] H. Volz, H. Kowarsch, J. Organomet. Chem. 136 (1977) C27.
[18] J.A. Ewen, R.L. Jones, M.J. Elder, A.L. Rheingold, L.M. Liable-Sands, J. Am. Chem. Soc. 120 (1998) 10786.
[19] J.A. Ewen, M.J. Elder, R.L. Jones, A.L. Rheingold, L.M. Liable-Sands, R.D. Sommer, J. Am. Chem. Soc. 123 (2001) 4763.
[20] A.N. Ryabov, D.V. Gribkov, V.V. Izmer, A.Z. Voskoboynikov, Organometallics 21 (2002) 2842.
[21] C. De Rosa, F. Auriemma, A. Di Capua, L. Resconi, S. Guidotti, I. Camurati, I.E. Nifant'ev, I.P. Laishevstsev, J. Am. Chem. Soc. 126 (2004) 17040.
[22] I.E. Nifant'ev, I.P. Laishevstsev, P.V. Ivchenko, I.A. Kashulin, S. Guidotti, F. Piemontesi, I. Camurati, L. Resconi, P.A.A. Klusener, J.J.H. Rijsemus, K.P. de Kloe, F.M. Korndorffer, Macromol. Chem. Phys. 205 (2004) 2275.
[23] C. Grandini, I. Camurati, S. Guidotti, N. Mascellani, L. Resconi, I.E. Nifant'ev, I.A. Kashulin, P.V. Ivchenko, P. Mercandelli, A. Sironi, Organometallics 23 (2004) 344.
[24] L. Resconi, S. Guidotti, I. Camurati, R. Frabetti, F. Focanate, I.E. Nifant'ev, I.P. Laishevstsev, Macromol. Chem. Phys. 206 (2005) 1405.
[25] D.A. Kissounko, M.V. Zabalov, Yu.F. Oprunenko, D.A. Lemenovskii, Rus. Chem. Bull. 49 (2000) 1282.
[26] D.A. Kisun'ko, M.V. Zabalov, Yu.F. Oprunenko, E.M. Myshakin, D.A. Lemenovskii, Russ. J. Gen. Chem. 71 (2001) 1751.
[27] D.A. Kisun'ko, M.V. Zabalov, Yu. F. Oprunenko, D.A. Lemenovskii, Russ. J. Gen. Chem. 74 (2004) 105.
[28] O. Meth-Cohn, S. Gronowitz, Acta Chem. Scand. 20 (1966) 1733.
[29] H. Volz, H. Kowarsch, Tetrahedron Lett. 48 (1976) 4376.
[30] J.A. McCleverty, G. Wilkinson, in: R.J. Angelici (Ed.), Inorganic Syntheses, vol. 28, John Wiley & Sons, New York, 1990, p. 84.
[31] C. Adamo, V. Barone, J. Chem. Phys. 116 (2002) 5933.
[32] J.P. Perdew, K. Burke, M. Ernzerhof, Phys. Rev. Lett. 77 (1996) 3865.
[33] M. Ernzerhof, G.E. Scuseria, J. Chem. Phys. 110 (1999) 5029.
[34] D.N. Laikov, Chem. Phys. Lett. 281 (1997) 151.
[35] D.N. Laikov, Yu.A. Ustynyuk, Russ. Chem. Bull. 54 (2005) 820.

[36] A. Ceccon, P. Ganis, M. Imhoff, F. Manoli, S. Santi, A. Venzo, J. Organomet. Chem. 577 (1999) 167.
[37] S. Bi, B. Wang, Z. Zhang, S. Zhu, Chem. Phys. Lett. 426 (2006) 192.
[38] J.W. Faller, R.H. Crabtree, A. Habib, Organometallics 4 (1985) 929.
[39] C. Bonifaci, A. Ceccon, S. Santi, C. Meali, R.W. Zoellner, Inorg. Chim. Acta 240 (1995) 541.